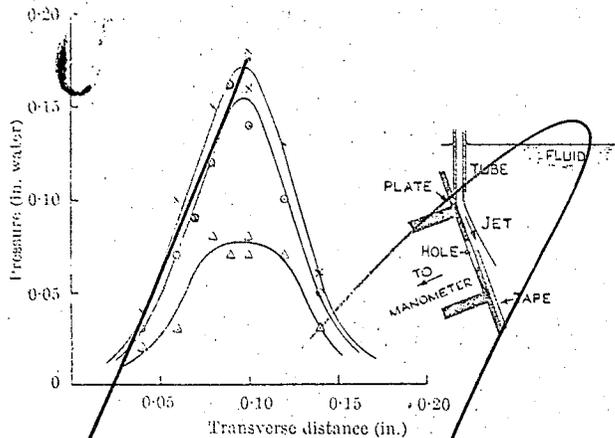Fig. 6. Transverses across jets on plate. ×, Water; ○, 60 p.p.m. guar; △, 30 p.p.m. 'Polyox'

away from the wall, accumulations of 'dead' fluid occur, and intermittently erupt into the outer boundary layer, provoking turbulent mixing. It seems not unlikely that viscoelastic effects would tend to counter this vortex motion at the wall. Thus viscoelastic jets impinging on a wall tend if anything to be deflected up away from it, as is evidenced by the reduced friction of Fig. 6 and as can also be seen by viewing the jets of Fig. 5 from the side. Conversely the slower-moving fluid may well tend to be held on to the wall, and thus prevented from erupting.

This process might minimize the turbulent mixing and generation of turbulent eddies.

To conclude, we may claim that although the drag-reducing and turbulence-damping properties of dilute long-chain-molecule solutions may seem paradoxical at first sight, since the density and steady-flow viscosity are little different from those in water, the viscoelastic characteristics which the solutions seem to possess provide at least a partial explanation.

I have been helped in my work by conversation and correspondence with many people, especially the following: Mr. P. Bradshaw, Mr. S. C. Crow, Dr. J. W. Hoyt, Dr. J. I. Jones, Prof. J. L. Lumley, Prof. J. G. Oldroyd, Dr. A. M. Patterson, Dr. J. R. A. Pearson, Dr. B. E. Read, Prof. W. C. Reynolds and Dr. D. H. Whiffen.

[1] Hoyt, J. W., and Fabula, A. G., paper presented at the ONR-Skipsmodell-tanken, Fifth Symp. Naval Hydrodynamics, Bergen, Norway (Sept. 1964).
[2] Vogel, W. M., and Patterson, A. M., paper presented at the ONR-Skips-modelltanken, Fifth Symp. Naval Hydrodynamics, Bergen, Norway (Sept. 1964).
[3] Shaver, R. G., and Merrill, E. W., Amer. Inst. Chem. Eng. J., 5, 181 (1959).
[4] Dodge, D. W., and Metzner, A. B., Amer. Inst. Chem. Eng. J., 5, 189 (1959).
[5] Ripken, J. F., and Pilch, M., Univ. Minnesota, St. Anthony Falls Hydraulic Lab., Tech. Paper, No. 42, B (April 1963).
[6] Savins, J. G., Soc. Petroleum Eng. J., 4, 203 (1964).
[7] Sinclair Wells, C., paper presented at the A.I.A.A. Aerospace Sci. Meeting, New York (Jan. 1964).
[8] Metzner, A. B., and Park, M. G., J. Fluid Mech., 20, 291 (1964).
[9] Fröhlich, H., and Sack, R., Proc. Roy. Soc., A, 185, 415 (1946).
[10] Oldroyd, J. G., Proc. Roy. Soc., A, 245, 278 (1958).
[11] Frater, K. R., J. Fluid Mech., 20, 369 (1964).
[12] Runstadler, P. W., Kline, S. J., and Reynolds, W. C., Stanford Univ. Mech. Eng. Dept. Rep. No. AFOSR/TN/5241 (June 1963).

BIOPHYSICS OF PLANT GROWTH IN AN ELECTROSTATIC FIELD

By L. E. MURR

Department of Engineering Mechanics, Solid State Microstructures Research Laboratory,
Pennsylvania State University

EXPERIMENTAL investigations of grass plant growth in an electrostatic field over the past two years[1-3] have revealed that it is impeded, and in certain cases lethal damage occurs. The electric field damage has been shown to be related to an enzymatic stimulation[2], but it has not been defined in detail. In the present investigation, bio-electronic processes in the initiation of plant-cell damage are described, and the field activation mechanism is defined in terms of a corona-type charge density process.

Investigations on orchard grass and grain sorghum were undertaken in an electrostatic environment generated by the system shown schematically in Fig. 1. Growing times, moisture requirements, and the control of related growth variables were identical to those employed in previous work[1]. The damage response for grain sorghum in this electrostatic environment, as shown in Fig. 2, was nearly identical to that reported for seedling orchard grass[1]. It will be observed that the damage response shown is computed on the basis of what is defined as the static reference potential gradient,

$$E_1 = \frac{V_0}{d} \tag{1}$$

where E_1 is the reference potential gradient in kV/m, V_0 is the voltage applied to the electrostatic environment, and d is the total distance from the soil surface to the anode plate as indicated in Fig. 1. The validity of this field equation with respect to this particular experimental system, when the plant matter is neglected, has already been shown[4]. The basis for the use of equation (1) to describe the field conditions of each experiment is therefore to consider a volume effect of the entire active electrostatic environment. In such a case, the presence of the

grass plants in the environment is assumed to be nearly negligible dielectrically, and the field response is computed as shown in equation (1).
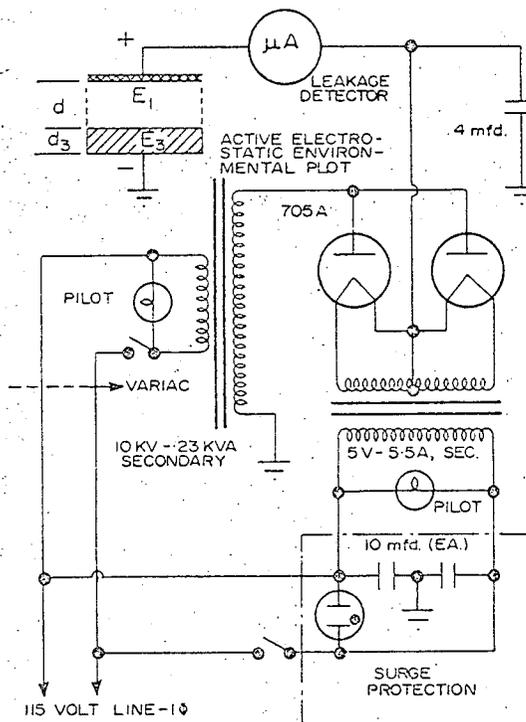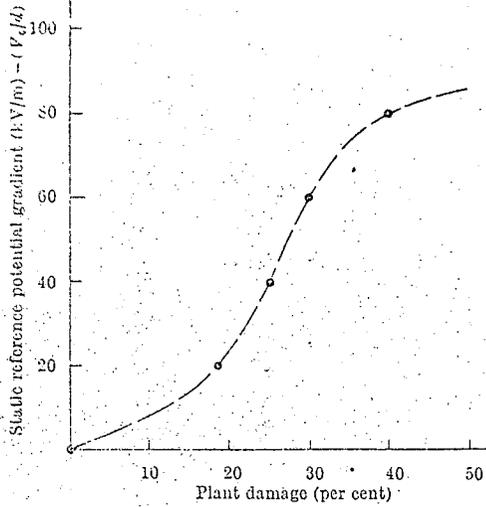

Fig. 1. Electrostatic power supply

Fig. 2. Grain sorghum plant growth response under various reference potential gradients based on an average of two dry weight comparisons of activated and control plants at each potential gradient condition
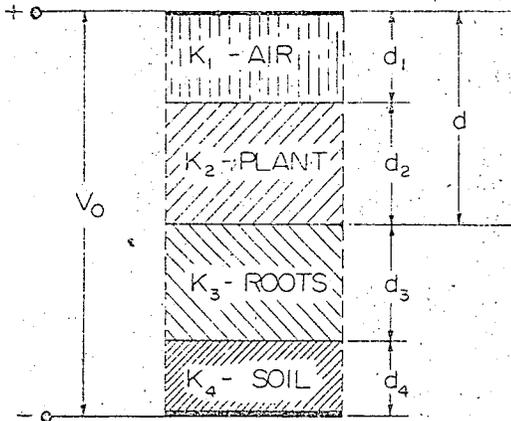

Fig. 3. Dielectric column analogy—schematic

Experimental results[1-3] have indicated, however, that each plant is individually affected by the electric field action, and that the field action is a dynamic rather than a static response. This implies simply that, electrostatically, each plant must be considered on the basis of a column dielectric. This analogy is shown schematically in Fig. 3. In this model, which is perhaps rather crude in some respects, both the upward growth of the plant and the propagation of roots into the soil are considered. We will initially make the assumption that the electric flux is normal at the interfaces of the dielectrics so that we have essentially:

$$D_1 = D_2 = D_3 = D_4 \tag{2}$$

where:

$$D_n = \varepsilon_0 K_n E_n \tag{3}$$

D_n being defined as the electric flux density, ε_0 is a constant, K_n is defined as the relative dielectric constant for the material in a region n, and E_n is the potential gradient in a region n. For a potential difference of V_0 between the dielectric column of Fig. 3, we also have:

$$V_0 = \sum_{n=1}^{n=4} E_n d_n \tag{4}$$

and performing the summation:

$$V_0 = E_1 d_1 + E_2 d_2 + E_3 d_3 + E_4 d_4 \tag{5}$$

An equation describing the electric potential gradient in the air-space region ($n = 1$) immediately above the plant leaf is then obtained by considering equations (2)

and (3) and the proper substitution into equation (5), obtaining:

$$V_0 = E_1 \left[d_1 + K_1 \left(\frac{d_2}{K_2} + \frac{d_3}{K_3} + \frac{d_4}{K_4} \right) \right] \tag{6}$$

Equation (6) can be simplified somewhat by considering the fact that the relative dielectric constant for air, K_1, is unity; and by assuming that the relative dielectric constant for the root material is probably the same as that for the plant material, that is, $K_2 \equiv K_3$. Rewriting, we then have:

$$V_0 = E_1 \left(d_1 + \frac{d_2}{K_2} + \frac{d_3}{K_2} + \frac{d_4}{K_4} \right) \tag{7}$$

Observations of root growth in all experiments have revealed the fact that by the time the plants have attained a height of 1–2 in. above the soil, the roots have penetrated the soil to the cathode. Since this occurred before leaf damage was observed to occur, it will be assumed that, in considering the dynamic field response, we can
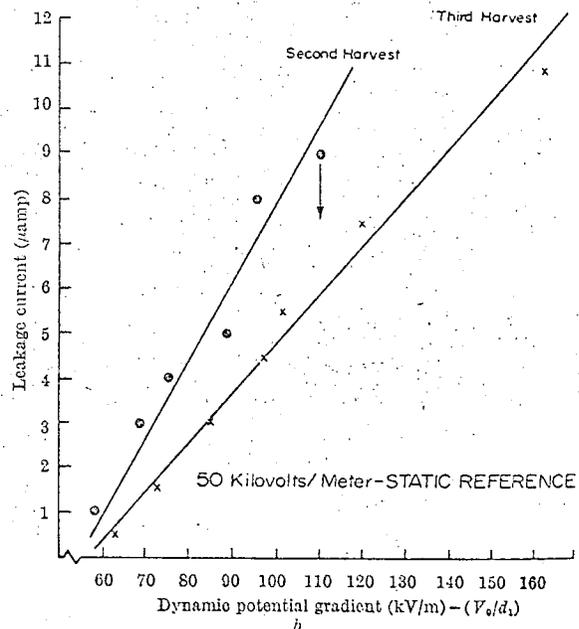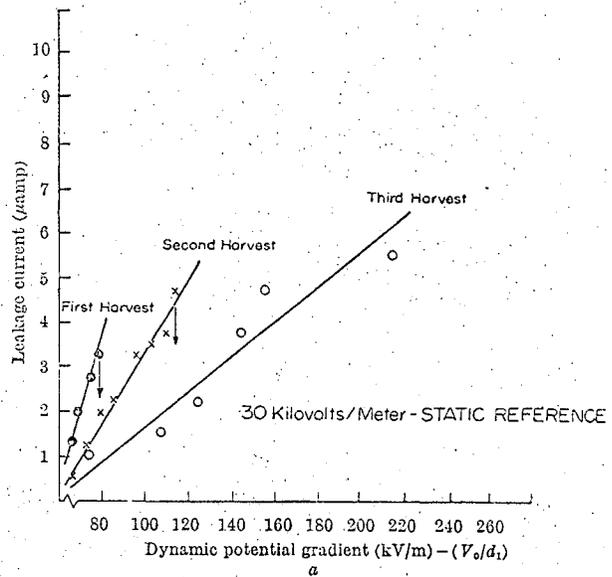

Fig. 4. Leakage current response for orchard grass grown and gathered in an electrostatic field. (a) Growth-regrowth response at 30 kV/m static reference potential gradient. (b) Growth-regrowth response at 50 kV/m static reference potential gradient

Fig. 5. Photograph of grain sorghum plants in the active environment operated at 80 kV/m static reference potential gradient after 10 days from planting of seeds. Double and repeated images at (A) and (D) are indicative of the field oscillation of the damaged leaves. Leaf damage is very apparent at (B) and (C)

let $d_4 = 0$ as would be the case for total root propagation along the dielectric column of Fig. 3. Thus, equation (7) would become:

$$V_0 = E_1\left(d_1 + \frac{d_2}{K_2} + \frac{d_3}{K_2}\right) \qquad (8)$$

Further simplification of equation (8) is possible since the experimental conditions have been defined by:

$$\left[\begin{array}{c} Nd_3 = (d_1 + d_2) \\ N \geqslant 1 \end{array}\right] \qquad (9)$$

Thus, substitution of the conditions of equation (9) into equation (8) results in:

$$V_0 = E_1\left[d_1\left(1 + \frac{1}{NK_2}\right) + d_2\left(\frac{1}{K_2} + \frac{1}{NK_2}\right)\right] \qquad (10)$$

Experiments have also shown that the relative dielectric constant, K_2, for the grass plants considered in this investigation, and grasses in general, is of the order of 1,000 or greater[5]. This would then imply the following approximations:

$$\left[\begin{array}{c} \left(1 + \frac{1}{NK_2}\right) \cong 1 \\ \left(\frac{1}{K_2} + \frac{1}{NK_2}\right) \rightarrow 0 \end{array}\right] \qquad (11)$$

On substituting these final conditions, equation (11), into equation (10), we observe the very simple relationship descriptive of the potential gradient in the air space above the growing plant:

$$E_1 \cong \frac{V_0}{d_1} \qquad (12)$$

It will be noted here that (12) is quite similar to (1). Equation (12) is, however, a dynamic equation, while (1) represents a static definition of the electric field intensity.

When the dynamic equation (12) was employed in plotting the leakage current detected in the electrostatic system (see Fig. 1), the results indicated in Fig. 4 were obtained for orchard grass. The change in slope observed for successive gatherings is indicative of a change in the current density for some arbitrary value of the dynamic potential gradient. This occurs because the leaf geometry is changed, for example with clipping and regrowth; initially the leaves were pointed, resulting in a charge density maximum, and, after clipping, the leaves were effectively flattened and became broadened. Successive clipping then continued to flatten the leaves while the blade width increased with regrowth. It is perhaps of interest to point out that the leakage current was detected

only at the onset of leaf-tip damage, as previously defined[1]. The tip damage activation current is observed from Fig. 4 to be approximately 5×10^{-7} amp. In the early experiments of Blackman and Legg[6], it was observed that plant growth increases disappeared at what they described as an optimum current intensity of 10^{-6} amp.

Several examples of dynamic properties of the electrostatic environment were observed which, along with data similar to those of Fig. 4, suggested that a corona-type field activation process is responsible for the initiation of epidermal leaf damage. In one case, the damaged leaf tips were observed to vibrate in the electrostatic environment. This vibration, as well as leaf damage, is shown in the photograph of Fig. 5. In addition to this field vibration phenomenon, the damaged leaf tips were observed to have a negative charge with respect to the normal positive sense illustrated in the sketch in Fig. 6. This phenomenon is unmistakably indicative of field polarization, and the concentration of charged bodies in the damaged leaf tip. This effect was observed simply by holding a plastic probe near the damaged leaf tip and observing that the tip was strongly repelled. Undamaged tips as well as the control plant leaves were strongly attracted to the probe. Although this effect seems to suggest the presence of ionic radicals in the damaged leaf tips, the presence of polarized molecules such as metallo-enzymes can also account for such behaviour.
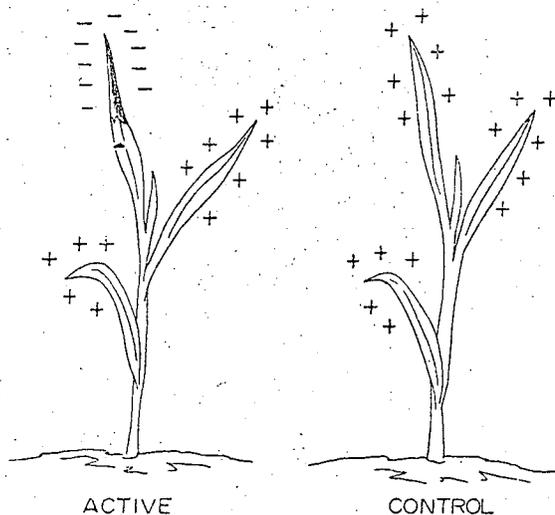

Fig. 6. Normal (control) and damaged leaf polarity as observed for grain sorghum plants at all relative potential gradients where leaf damage was observed

Local field effects associated with the initiation of plant damage were further supported by experimental results such as those shown in Fig. 7. In the graphs in Fig. 7, the static reference potential gradient as computed by equation (1) is plotted against what is defined as a critical damage ratio (δ_2/d), where δ_2 is the average plant height at which leaf damage was detected, and d is the total soil-surface to anode distance as indicated in Fig. 3. Fig. 7 shows two effects: (a) that the regrowth plant damage is shifted in a manner identical with the slope changes observed in Fig. 4, and (b) that the theoretical destruction gradient in the natural environment, based on the condition $\delta_2/d = 0$, is observed to be of the order of 110–130 kV/m by extrapolation of the curves.

One final comparison of the static and dynamic field gradients associated with the initiation of plant leaf damage is shown in Fig. 8. This offers a means of associating the experimental damage phenomena observed, with naturally occurring electrical phenomena. Considering the semi-log plot for the orchard grass and the
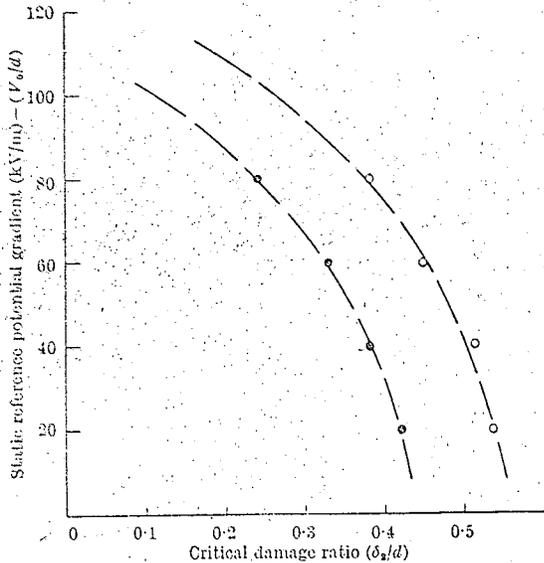
Fig. 7. Electrostatic field damage response for the initial growth (◉) and first gathering regrowth (◯) of grain sorghum plants. The numerator (δ_1) of the critical damage ratio represents the average height of the leaf tip above the soil surface at which damage was observed. The experimental plant population in all instances was greater than 30 plants, most of which developed several damaged leaves before gathering
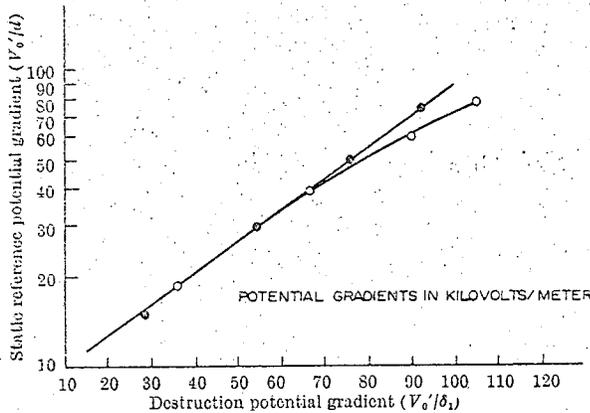

Fig. 8. Electro-dynamic response for orchard grass (◉) and grain sorghum (◯) based on averages of observations of the plant-leaf height at the onset of electric-field damage

slight deviation from this curve for the grain sorghum, the following equation for this curve is obtained:

$$\left(\frac{V_0{}'}{\delta_1}\right) = 10^2 \left[\log\left(\frac{V_0{}'}{d}\right) - 1\right] \tag{13}$$

Now, since $d = \delta_1 + \delta_2$, we can substitute this condition back into equation (13) to obtain:

$$\delta_2 = \left\{ d - \frac{V_0{}'}{10^2 \left[\log\left(\dfrac{V_0{}'}{d}\right) - 1\right]} \right\} \tag{14}$$

Observe that δ_2 with reference to the natural environment is the height at which plants will be damaged by some terrestrial field gradient. In this same sense, we will consider that d in equation (14) is the total distance from the effective terrestrial anode to the Earth's surface. Thus, we can see that $d \gg \delta_2$; and by substitution of this condition back into equation (14) we can write the following approximation:

$$d \cong \frac{V_0{}'}{10^2 \left[\log\left(\dfrac{V_0{}'}{d}\right) - 1\right]} \tag{15}$$

Let us now consider storm activity where we can be assured that high potential gradient levels might exist.

In such instances, the coiling height will be substituted for d in equation (15), and is of the order of 6 km (ref. 7). Equation (15) then transforms into the transcendental-type equation:

$$\log V_0{}' - 1\cdot7 \times 10^{-6} \, V_0{}' \cong 4\cdot8 \tag{16}$$

the solution of which is $V_0{}' \cong 9 \times 10^4$ kV. This value represents the critical damage voltage required under the assumed storm front which could theoretically initiate plant damage. Dividing this value by the cloud cover height, $d = 6$ km then results in a critical potential gradient of approximately 15 kV/m. This result is indeed of interest since it is known that normal cloud to ground field gradients during thunderstorms are 30 kV/m (ref. 7), or about twice the theoretically necessary field intensity to initiate plant-leaf damage.

One is now led to ask: if the preceding analysis is valid, why has plant damage not been observed following such storms? The answer, perhaps simply enough, is that storm durations are not sufficient to initiate complete and observable damage. However, in the case of severe dust storms and other related high-charge density phenomena, one might expect damage to occur by virtue of the exceedingly large field intensities developed. It seems, indeed, that this is exactly what has been reported by Miller[8], who relates observations of cereal damage in the great plains of the United States.

I have attempted to show in this article that the physical and electrical properties of the electrostatic system can be significantly related to the biological damage observed in grass plants. With reference to the experimental evidence presented, it is apparent that leaf damage is indeed associated with direct field or corona-type stresses induced in the leaf epidermis. This phenomenon is further enhanced by polarization actions of plant bio-substances. There seems to be no need for a physiological response to accompany the field stress as previously proposed[1], since the dynamic field intensities calculated at the time leaf damage was observed are more than sufficient to cause epidermal deterioration by a type of field evaporation of organic molecules composing the outer cells.

At the onset of this field-initiated leaf damage, the respiratory mechanism of the plant is taxed to supply an uncontrollable abundance of biochemical substances, enzymes and related metallo-enzymes. Previous experimental work has shown this in the case of orchard grass[2], and Table 1 shows a similar microchemical analysis for grain sorghum. There is a significant increase in phosphorus content in the active grain sorghum plants which was not detected for orchard grass. The difference might possibly indicate a higher degree of polarization in the grain sorghum due to its different physiology.

Table 1. SPECTROSCOPIC ANALYSIS OF GRAIN SORGHUM PLANTS

Sample	P (% dry weight)	K	Ca	Mg	Fe (p.p.m. dry weight)	Zn	Al	Mn	Cu
40 kV/m active	0·610	3·69	0·86	0·340	181	78	116	377	23
40 kV/m control	0·470	3·69	1·05	0·300	163	71	69	377	24
60 kV/m active	0·447	3·45	1·08	0·411	288	80	180	720	36
60 kV/m control	0·381	3·33	0·96	0·318	230	70	126	708	32
80 kV/m active	0·710	3·33	0·90	0·330	233	79	145	470	30
80 kV/m control	0·434	3·69	0·97	0·310	163	61	75	659	27

[1] Murr, L. E., Nature, 200, 490 (1963).
[2] Murr, L. E., Nature, 201, 1305 (1964).
[3] Murr, L. E., Proc. Penn. Acad. Sci., 37, 109 (1963).
[4] Murr, L. E., Proc. Penn. Acad. Sci., 36, 25 (1962).
[5] Murr, L. E., paper to be presented to the Pennsylvania Academy of Science (March, 1965).
[6] Blackman, V. H., and Legg, A. T., J. Agric. Sci., 14, 268 (1924).
[7] Bewley, L. V., Travelling Waves on Transmission Systems, 106 (Dover, New York, 1963).
[8] Miller, E. C., Plant Physiology, 1085 (McGraw-Hill, New York, 1938).